HHS Public Access

Author manuscript

*Nat Chem*. Author manuscript; available in PMC 2014 December 01.

Published in final edited form as:

*Nat Chem*. 2014 June ; 6(6): 542–552. doi:10.1038/nchem.1924.

# mitochondrial pathway for biosynthesis of lipid mediators

**Yulia Y. Tyurina**[1,*], **Samuel M. Poloyac**[3], **Vladimir A. Tyurin**[1,2], **Alexander A. Kapralov**[1,2], **Jianfei Jiang**[1,2], **Tamil Selvan Anthonymuthu**[1,4], **Valentina I. Kapralova**[1,2], **Anna S. Vikulina**[1,2,7], **Mi-Yeon Jung**[1,2], **Michael W. Epperly**[5], **Dariush Mohammadyani**[6], **Judith Klein-Seetharaman**[8], **Travis C. Jackson**[4], **Patrick M. Kochanek**[4], **Bruce R. Pitt**[2,6], **Joel S. Greenberger**[5], **Yury A. Vladimirov**[7], **Hülya Bayır**[1,4,*], and **Valerian E. Kagan**[1,2,*]

[1]Center for Free Radical and Antioxidant Health, Swanson School of Engineering, University of Pittsburgh, Pittsburgh PA 15213, USA

[2]Department of Environmental Health, Graduate School of Public Health, Swanson School of Engineering, University of Pittsburgh, Pittsburgh PA 15213, USA

[3]Department of Pharmaceutical Sciences, School of Pharmacy, Swanson School of Engineering, University of Pittsburgh, Pittsburgh PA 15213, USA

[4]Department of Critical Care Medicine, Safar Center for Resuscitation Research, Swanson School of Engineering, University of Pittsburgh, Pittsburgh PA 15213, USA

[5]Department of Radiation Oncology, School of Medicine, Swanson School of Engineering, University of Pittsburgh, Pittsburgh PA 15213, USA

[6]Department of Bioengineering, Swanson School of Engineering, University of Pittsburgh, Pittsburgh PA 15213, USA

[7]Department of Biophysics, MV Lomonosov Moscow State University, Moscow, Russia

[8]Division of Metabolic and Vascular Health, University of Warwick, Coventry CV4 7AL, UK

## Abstract



*Correspondence to: Yulia Tyurina, yyt1@pitt.edu or Hülya Bayır, bayihx@ccm.upmc.edu or Valerian Kagan, kagan@pitt.edu.

**Author contributions**

Y.Y.T. designed experiments, performed MS analysis of cardiolipin and its oxidation and hydrolysis products *in vivo* and *in vitro,* and co-wrote the maniuscript, S.M.P. performed MS analysis of oxygenated species of arachidonic acid, V.A.T. performed experiments on cardiolipin hydrolysis by $LpPLA_2$ and MS analysis of cardiolipin and its hydrolysis products in small intstine and cells, A.A.K. performed experiments on peroxidase activity of cytc/CL complexes, J.J. performed the experiments on knocking down t-cyt *c*, T.S.A., and V.I.K. participated in MS analysis of cardiolipin and its oxidation and hydrolysis products, A.S.V., and M.Y.J. performed cell and mitochondria experiments, D.M., and J.K.S. perfomed computational analysis of s-cyt *c* and t-cyt *c*, M.W.E., and J.S.G. contributed to the design and performance of the *in vivo* experiment (whole body irradiation), T.C.J. and P.M.K. participated in the design and performance of the in vitro experiments with neurons and astrocytes, Y.A.V., and B.R.P. participated in discussion of the results on LC/MS and aspects of the work with the hydrolysis of $CL_{ox}$, H.B. contributed to the formulation of the initial concept of the study, designed and participated in the performance of the *in vivo* experiment (controlled cortical impact), co-wrote the maniuscript, V.E.K. suggested the idea, designed the study, wrote the manuscript. All authors discussed the results and commented on the manuscript.

**Competing financial interests:** The authors declare no competing financial interests.

The central role of mitochondria in metabolic pathways and in cell death mechanisms requires sophisticated signaling systems. Essential in this signaling process is an array of lipid mediators derived from polyunsaturated fatty acids. However, the molecular machinery for the production of oxygenated polyunsaturated fatty acids is localized in the cytosol and their biosynthesis has not been identified in mitochondria. Here we report that a range of diversified polyunsaturated molecular species derived from a mitochondria-specific phospholipid, cardiolipin, are oxidized by the intermembrane space hemoprotein, cytochrome c. We show that an assortment of oxygenated cardiolipin species undergoes phospholipase $A_2$-catalyzed hydrolysis thus generating multiple oxygenated fatty acids, including well known lipid mediators. This represents a new biosynthetic pathway for lipid mediators. We demonstrate that this pathway including oxidation of polyunsaturated cardiolipins and accumulation of their hydrolysis products – oxygenated linoleic, arachidonic acids and monolyso-cardiolipins – is activated *in vivo* after acute tissue injury.

Mitochondria of eukaryotic cells contain machinery capable of oxidizing substrates in a coupled enzymatic and electrochemical process that effectively generates energy in the form of ATP. In addition to the powerhouse function, mitochondria are now viewed as the major regulatory platform involved in numerous intra- and extracellular metabolic and physiological pathways – from synthesis of major intracellular biomolecules to assembly of inflammasomes, immune responses, generation of reactive oxygen species, dynamic regulation of their own organization via fission/fusion and mitophagy as well as control and execution of apoptotic and necrotic cell death[1]. Although there is an intuitive necessity for the existence of specific signals for mitochondrial communications – the identification of these signals has not been fully achieved. An array of lipid mediators, with diversified and potent signaling effects on the normal homeostasis and responses to stress and disease, are generated through oxygenation of free polyunsaturated fatty acids (PUFA). Molecular machinery involved in the production of these bioactive oxygenated compounds has been mostly assigned to the cytosol[2]. Surprisingly, mitochondria have not been identified as a site of lipid mediators biosynthesis[3].

The rate limiting step in the production of lipid mediators is the availability of oxidizable PUFA[4]. Normally esterified into cellular (phospho)lipids, free PUFA are released by $Ca^{2+}$-dependent phospholipases $A_2$ ($PLA_2$) and act as substrates for oxygenation reactions by several enzymes, including, cyclooxygenases (COX), lipoxygenases (LOX), cytochrome P450 isoforms, and peroxidases[5]. A plethora of lipid regulators including prostaglandins, prostacyclins, thromboxanes, resolvins, protectins, maresins, leukotrienes, lipoxines, lipoxenes, levulo-glandins, among others, with multitude of physiologic effects are formed[6, 7]. Notably, the major precursor of lipid mediators, phosphatidylserine (PS)[8], is lacking from mitochondria[9]. The majority of phospholipids constituting the inner and outer mitochondrial membranes (IMM and OMM) are manufactured outside of the organelle, with a notable exception of mitochondria-specific cardiolipin (CL). CL (1,3-bis(sn-3'-phosphatidyl)-sn-glycerol) is structurally unique as it contains two phosphatidyl groups linked to a glycerol backbone and four fatty acyl chains. With about 20 different, mostly PUFA residues available for esterification, the diversity of CLs and its oxygenated species may be very high thus making it an exceptionally good source of lipid mediators.

The final rate-limiting step in the production of CL takes place in the IMM to which the newly synthesized CL molecules are sequestered thus generating characteristic CL asymmetry[10]. Collapse of CL asymmetry and accumulation of its oxygenated products, have been identified as essential early steps of apoptosis culminating in the release of pro-apoptotic factors[11]. CL oxygenation is catalyzed by CL/cytochrome *c* (cyt *c*) complexes that act as a potent CL-specific peroxidase[11] via an enzymatic mechanism similar to that of COX-2 catalyzed oxygenation of arachidonic acid (AA)[12]. Given that cyt *c*-driven reactions yield a highly diversified set of oxidized CL ($CL_{ox}$) products, including different stereo-isomers with hydroperoxy-, hydroxy-, epoxy- and oxo-functionalities[13, 14], we hypothesized that mitochondrial CLs can be a source of bioactive lipid mediators. While lipid mediators, particularly eicosanoids, have been implicated in the regulation of intrinsic and extrinsic apoptotic pathways[15], mitochondria have not been associated with their biosynthesis. Here we report that CL is oxidized to highly diversified polyunsaturated molecular species by cyt *c* thereby, representing a new biosynthetic pathway for lipid mediator production. A rich assortment of $CL_{ox}$ species subsequently undergoes hydrolysis by $Ca^{2+}$-independent $iPLA_2\gamma$ thus generating multiple oxygenated FAs ($FA_{ox}$) that include well known lipid mediators as well as oxygenated species of lyso-CLs with yet to be determined biological functions.

## RESULTS

### Selective oxidation and hydrolysis of CL in mouse small intestine

To ascertain whether mitochondrial CL can be a source of lipid mediators we performed lipidomics analysis of two different tissues - small intestine and brain - after whole body irradiation (WBI) and controlled cortical impact (CCI), respectively. In small intestine (a radiosensitive tissue) of C57BL6 mice exposed to 10 Gy of WBI, LC/MS analysis revealed: i) a decrease of oxidizable polyunsaturated CL molecular species (Fig. 1a), ii) generation of $CL_{ox}$ (Fig.1b) and iii) accumulation of mono-lyso-cardiolipins (mCLs) (Fig. 1c) and $FA_{ox}$ (Fig. 1d). $CL_{ox}$ were mainly represented by molecular species containing one, two and three additional oxygen atoms and their structures were confirmed by MS/MS analysis (Fig. 1b). While mCLs mainly included non-oxidized molecular species, both mono- and di-oxygenated species of mCL ($mCL_{ox}$), particularly with mono- and di-oxygenated LA, were also detected (Supplementary Table S1, Supplementary Fig. S1) whereby the mono-oxygenated mCL derivatives were predominant (Fig. 1c). Quantitatively, the amount of detectable $CL_{ox}$ (0.12 ± 0.05 pmol/nmol of total phospholipids) was ~2.5 times lower than the level of mCL (0.30 ± 0.18 pmol/nmol of total phospholipids). This indicates that the hydrolysis reactions – possibly catalyzed by $Ca^{2+}$-independent $iPLA_2\gamma$ – were effective in converting $CL_{ox}$ into mCLs. The major $FA_{ox}$ species – mostly mono-oxygenated LA-derivatives - were 9-HODE and 13-HODE (Fig 1d). In addition, 9-KODE, 13-KODE, 9-HpODE, 13-HpODE, 12-HETE, 15-KETE, 15-HETE were also detectable albeit in significantly smaller amounts (Supplementary Fig. S2, Supplementary Table S2).

To ascertain whether $iPLA_2\gamma$ might be accountable for the hydrolysis of $CL_{ox}$ leading to the generation of mCLs, we utilized 6E- (bromoethylene)tetrahydro-3R- (1-naphthalenyl)-2H-pyran-2-one, (R)-bromoenol lactone ((R)-BEL), an inhibitor of $Ca^{2+}$-independent $iPLA_2\gamma$ *in vivo*[16]. We confirmed that (R)-BEL did not inhibit peroxidase activity of cyt c/CL

complexes (Supplementary Table S3). (R)-BEL blocked the irradiation-induced accumulation of mCL by 94.9±0.7%. Notably, irradiation induced accumulation of two major lyso-phosphatidylcholines (LPC) (16:0-LPC and 18:0-LPC) was not significantly affected by (R)-BEL (data not shown). The amount of detectable $CL_{ox}$ in the small intestine of mice pretreated with (R)-BEL and exposed to WBI was estimated as 0.29 ± 0.15 pmol/nmol of total phospholipids, a ~2.5-fold increase *vs.* its content in the absence of the inhibitor. Thus $iPLA_2\gamma$ has been mainly responsible for the hydrolysis of $CL_{ox}$ and the production of mCL. Simultaneously, the total amount of released $FA_{ox}$ was inhibited by 67.3±7.2%. In particular, 12-HETE and 15-HETE concentrations in irradiated intestinal samples from (R)-BEL treated animals were 45.7±16.0% and 76.3±28.0% of untreated irradiated intestinal samples. Expectedly, the decrease of oxidizable CL species was not significantly affected by (R)-BEL (data not shown). Overall, these data emphasize the major role of $Ca^{2+}$-independent $iPLA_2\gamma$ in the generation of mCLs and also reflect the likely involvement of other pathways – independent of $iPLA_2\gamma$ – in the formation of $FA_{ox}$.

We next compared the effects of a cocktail of several reportedly effective inhibitors of COX-, LOX- and cytochrome P450-driven conventional biosynthetic mechanisms for lipid mediators species versus their generation via CL-dependent pathways. Specifically, we tested the effects of the inhibitors of: i) COX-1 and -2 - piroxicam (4-hydroxy-2-methyl-N-2-pyridinyl-2H-1, 2-benzothiazine-3-carboxamide-1,1-dioxide); ii) LOX - licofelone (6-(4-chlorophenyl)-2,3-dihydro-2,2-dimethyl-7-phenyl-1H-pyrrolizine-5-acetic acid); and cytochrome P450 epoxygenase/12-HETE activity (CYP2C) - MS-PPOH (N-(methylsulfonyl)-2- (2-propynyloxy)-benzene-hexanamide))[17–20] on the formation of $FA_{ox}$ in the small intestine of irradiated mice. Because all three enzymes – COX, P450 and 5-LOX – are iron-containing proteins of which the former two are hemoproteins, we assessed the effects of inhibitors on the catalytic peroxidase properties of cyt *c*/CL complexes *in vitro*. Within the range of concentrations corresponding to the doses applied in our *in vivo* experiments, these inhibitors did not suppress the peroxidase activity (Supplementary Table. S3). We found that the inhibitor cocktail partially decreased the levels of mono-oxygenated AA and oxo-LA compared with the group of mice that received no drugs before irradiation (Supplementary Table S4). The production of di-oxygenated LA did not appear to be affected by the mixture of inhibitors. This suggests that generation of lipid mediators from $CL/CL_{ox}$ is accomplished through the enzymatic reactions distinct from the known $Ca^{2+}$-dependent mechanisms realized via the release of free FAs and their subsequent oxygenation.

## Selective oxidation and hydrolysis of CL in rat brain

In rat brain, CLs were highly diversified and included mostly oxidizable polyunsaturated CLs (Fig. 2a). LC/MS analysis revealed that CCI caused depletion of oxidizable CLs containing LA, AA and docosahexaenoic (DHA) acids (Fig. 2a) and formation of $CL_{ox}$ (Fig. 2b) and its hydrolysis products: mCL (Fig. 2c) and $FA_{ox}$ (Fig. 2d). $CL_{ox}$ were mainly represented by species containing one and two additional oxygen atoms (Fig.2b). MS/MS analysis identified mono-oxygenated species of $CL_{ox}$ with either $LA_{ox}$ or $AA_{ox}$ (Fig. 2b). mCLs were represented by non-oxidized as well as oxidized $mCL_{ox}$ species (Fig. 2c, Supplementary Table S1, and Supplementary Fig. S3). The $CL_{ox}$ content was lower than the

amount of mCL: 0.10 ± 0.02 and 0.26 ± 0.08 pmol/nmol of total phospholipids, respectively. In addition, the oxygenated species of non-esterified LA and AA were produced (Fig. 2d, Supplementary Fig. S4), whereby several lipid mediators were identified such as 9-KODE, 13-KODE, 9-HODE, 13-HODE, 9,12,13,-KEpOME, 9-HpODE, 13-HpODE, 12-HETE, 15-HETE (Supplementary Table S2). Markedly smaller amounts of oxygenated DHA were also detected (Fig. 2d). Quantitatively, the CCI-induced loss of CL species containing PUFA was in good correspondence with the accumulation of $FA_{ox}$ (~5.1 and ~3.0 pmol/nmol of total phospholipids, respectively). This indicates that CL can be a source of CCI-induced production of $FA_{ox}$.

To ascertain whether the CL/$CL_{ox}$-dependent pathway may be cell type specific, we compared the responses of two types of brain cells – cortical neurons and one of the major components of glia, astrocytes, to a standard treatment with $H_2O_2$ *in vitro.* We found that neurons (Supplementary Fig. S5, Supplementary Table S5) contained more oxidizable polyunsaturated CL species than astrocytes (Supplementary Fig. S6, Supplementary Table S5). Accordingly, the amounts and speciation of $CL_{ox}$ after $H_2O_2$ exposure was also markedly richer in the former than in the latter (Supplementary Figs. S5 and S6). Similarly, the levels and diversification of mCLs was also significantly greater in neurons than in astrocytes (Supplementary Figs. S5 and S6).

## Generation of oxidized TLCL and its hydrolysis products in mitochondria

To further characterize pathways of CL peroxidation and hydrolysis we utilized C57BL6 mouse heart and liver mitochondria in which CL was accountable for ~15% of total phospholipids (Fig. 3). MS analysis demonstrated that oxidizable LA residues were present in all molecular species of CL (Supplemental Fig. S7). After exposure to a pro-oxidant, *t*-BuOOH, isolated mitochondria revealed the same pattern of characteristic CL changes as *in vivo*: i) decreased amounts of oxidizable CLs (Fig. 3a) accumulation of non-oxidized mCL (Fig. 3b) and $LA_{ox}$, (containing one and two oxygens) (Fig. 3c).

## Identification of cytochrome c as the catalyst of CL oxidation and hydrolysis

To directly assess the involvement of cyt *c* in CL peroxidation and hydrolysis products as a source of lipid mediators, we compared the production of mCL and $FA_{ox}$ in cyt $c^{+/+}$ and cyt $c^{-/-}$ mouse embryonic cells (MECs) during apoptosis triggered by non-oxidant (actinomycin D, ActD) or oxidant (*t*-BuOOH) stimuli (Fig. 4a). No significant differences were found in the total content and molecular speciation of CLs (approximately 3% of total phospholipids; 31.1±4.9 and 33.7±7.1 pmols CL/nmol total phospholipids, respectively) in cyt $c^{+/+}$ and cyt $c^{-/-}$ cells (Fig. 4b and Supplementary Fig. S8). Treatments with ActD or *t*-BuOOH caused a significant decrease of oxidizable polyunsaturated species of CL and accumulation of $CL_{ox}$ species with one and two oxygens in cyt $c^{+/+}$ cells - but not in cyt $c^{-/-}$ - cells (Fig. 4b and Supplementary Fig. S8). Quantitatively, the amounts of $CL_{ox}$ produced in cyt $c^{+/+}$ cells challenged with either ActD or *t*-BuOOH were increased 2.6- and 3.0 -times compared to untreated controls. Analysis of hydrolysis products revealed the presence of both oxidized and non-oxidized mCL (Fig. 4c) as well as oxygenated LA (Fig. 4d). Mono- and di-oxygenated molecular species of $mCL_{ox}$ were the predominant forms accumulating in cells upon the treatments (Fig.4c). Mono-oxygenated LA was the main product in ActD treated

cyt $c^{+/+}$ cells and was represented by a mixture of 9-HODE and 13-HODE (Fig. 4d). No significant increase in the levels of $CL_{ox}$ and CL hydrolysis products was detected in ActD and *t*-BuOOH treated cyt $c^{-/-}$ cells (Fig. 4). Notably, ActD or *t*-BuOOH triggered apoptosis in cyt $c^{+/+}$ cells as evidenced by a marked increase of PS externalization (Fig. 4a), whereas these pro-apoptotic effects were not found in cyt $c^{-/-}$ cells[11].

MECs express two isoforms of cyt c – somatic (s-cyt *c*) and testicular (t-cyt *c*)[21–23]. Western blot analysis established that t-cyt *c* was accountable for ~45% of the total cyt *c* in MECs (Supplementary Fig. S9). In cyt $c^{-/-}$ cells, the amount of t-cyt *c* was ~1.5 times lower than in cyt $c^{+/+}$ cells (0.83 ± 0.05 and 1.24 ± 0.08 ng/μg protein, respectively). As cyt $c^{-/-}$ cells rely more on glycolysis rather than mitochondrial respiration for ATP generation[24] they maintain lower levels of mitochondria. Indeed, Western blots showed that the levels of several mitochondrial marker proteins (COX-IV, MnSOD, TIM23) were ~46%–83% lower in cyt $c^{-/-}$ cells versus cyt $c^{+/+}$ cells (Supplementary Fig. S9). siRNA knock-down of the t-cyt *c* in cyt $c^{-/-}$ cells to ~50% of its content (Supplementary Fig. S9) did not affect the already low level of CL oxidation after ActD treatment. Similar to cyt $c^{-/-}$ cells the low level of mCL in cyt $c^{-/-}$ with knock-down t-cyt *c* remained unchanged after ActD exposure. These data suggest that t-cyt *c* is not a significant contributor to the generation of CL-driven lipid mediators.

## Hydrolysis of oxidized TLCL by mitochondrial $Ca^{2+}$-independent $PLA_2\gamma$

$Ca^{2+}$-independent $iPLA_2\gamma$ has been suggested as a likely candidate-catalyst capable to hydrolyze oxidized phospholipids in mitochondria[25]. To assess its role in the hydrolysis of $CL_{ox}$ species, we bio-synthesized (using cyt $c/H_2O_2$ system) and purified (to the level of 99% using LC/MS) oxidized tetralinoleoyl-cardiolipin ($TLCL_{ox}$ with 1–8 oxygens in four LA residues, see Supplementary Table S6 and Supplementary Fig. S10) and analyzed the products formed in the presence of a specific $iPLA_2\gamma$ inhibitor, (R)-BEL, in rat liver mitochondria (Fig. 3d). Mitochondria effectively hydrolyzed $TLCL_{ox}$ as evidenced by i) decrease of $TLCL_{ox}$ content (Fig. 3e) and ii) accumulation of oxygenated LA (with one and two oxygens) (Fig. 3f) as well as non-oxidized mCL and $mCL_{ox}$ (Fig. 3g,h). The hydrolysis of $TLCL_{ox}$ was effectively blocked by (R)-BEL (Fig. 3).

## Hydrolysis of oxidized TLCL by PAF acetylhydrolase

Mitochondria with externalized CL and/or $CL_{ox}$ as well as cyt *c* can be released into circulation during injury/disease process[26]. Thus circulating CL and $CL_{ox}$ can be a source of lipid mediators as well. Several phospholipases, including lipoprotein-associated $PLA_2$ ($LpPLA_2$) or platelet activating factor (PAF) acetylhydrolase (PAF-AH), have been shown to selectively hydrolyze oxidatively modified phospholipids to liberate $FA_{ox}$[27]. Recently, we have identified oxidized PS as a good substrate for Lp-$PLA_2$[28]. Because TLCL is the most predominant species of CL in circulation, we tested the ability of PAF-AH to release oxygenated FAs from $TLCL_{ox}$ produced in cyt *c* driven reaction (Supplementary Fig. S10). LC/MS analysis revealed accumulation of mCL containing both LA and $LA_{ox}$ (Figs. 5a, 5b, 5c), whereby $LA_{ox}$ was represented by molecular species with one and two oxygens (Fig. 5d). Markedly less effective hydrolysis was detected when non-oxidized TLCL was treated with PAF-AH (data not shown). Thus, PAF-AH predominantly hydrolyzes oxygenated

molecular species of CL to generate lipid signaling molecules formed in cyt *c* catalyzed reaction.

### Diversity of oxygenated FAs after hydrolysis of brain $CL_{ox}$ generated by cyt c/$H_2O_2$

The high diversification and enrichment with PUFA of brain lipids makes neuro-CLs particularly interesting as a source of lipid mediators generated via CL oxidation by cyt *c*. Indeed, we identified 56 major molecular species of CL in lipid extracts from mouse brain (Supplementary Table S7) of which 55 were highly oxidizable polyunsaturated CL containing one to four PUFAs (Fig. 6a). To establish molecular identity and stereospecificity of peroxidizable PUFA in neuro-CLs we employed a mixture of $PLA_1$ with $PLA_2$ and established that the dominant PUFAs of CL were represented by AA and LA (Fig. 6a). DHA, EPA, eicosatrienoic and octadecatrienoic acids were detected as well but in relatively lower abundance. Cyt *c*/$H_2O_2$ caused significant decrease of PUFA-containing molecular species of CL (Fig. 6b and Fig. 6c). By employing $PLA_1$ plus $PLA_2$ as a tool to liberate FA from both *sn*-1 and *sn*-2 positions of $CL_{ox}$ we identified by MS/MS analysis highly diversified molecular species of $LA_{ox}$ and $AA_{ox}$ (Fig. 6d) which included those detected in acutely injured tissues (brain after CCI and small intestine after WBI) (Supplementary Table S2) as well as in apoptotic cyt $c^{+/+}$ cells. In addition, oxidatively truncated FA molecular species were detected (Supplementary Table S2). Overall, 31 molecular species of $FA_{ox}$ have been identified as the products of brain $CL_{ox}$ hydrolysis.

## Discussion

Oxygenated free PUFAs – generated by a wide array of enzymes, including cyclooxygenases (COX-1 and COX-2), lipoxygenases (5-LOX, 12-LOX and 15-LOX) and cytochrome P450 isoforms [reviewed in[5, 7]] - have numerous physiological roles. The potent biological effects of lipid regulators necessitate the maintenance of very low endogenous levels of free PUFA. As a result, their availability is the rate-limiting step in the generation of lipid mediators[4]. Release of PUFA precursors from their phospholipid storage sites is achieved via action of $Ca^{2+}$-dependent phospholipases $A_2$ ($PLA_2$)[,30]. We have reported a new $Ca^{2+}$-independent pathway for selective generation of lipid mediators from a mitochondria-specific phospholipid, CL, whereby oxidation of FA residues is catalyzed by an intermembrane space protein, cyt *c*, directly in the esterified phospholipid. This is followed by hydrolysis of oxygenated CL species by two types of $PLA_2$ specific towards oxidatively modified phospholipids. This novel pathway disobeys the major dogmas of lipid mediator biochemistry with regards to: i) oxygenation of a phospholipid rather than a free FA as the reaction substrate, ii) mitochondrial – rather than cytosolic - localization- iii) an electron carrier cyt *c* – rather than an oxidase - as the reaction catalyst, iv) the final – rather than the initial – hydrolytic stage using oxygenated species of CL by $PLA_2$ to synthesize oxygenated PUFA, and v) $Ca^{2+}$-independent - rather than $Ca^{2+}$ dependent - nature of the pathway.

One can predict specific features of regulation of CL-dependent process that are markedly different from the “conventional” biosynthesis of oxygenated lipid mediators. The mitochondrial pathway is strictly dependent on the catalytic interactions between cyt *c* and

CL. However, these two participants have limited access to each other. The former is confined to the intermembrane space while the latter is "cloaked" almost exclusively in the inner mitochondrial membrane[31]. Importantly, ~15% of cyt *c* is believed to be hydrophobically bound to the IMM likely via its binding to CL in the outer leaflet of the IMM and cannot be removed from mitochondria, as occurs to the majority of cyt *c* upon treatment with high ionic strength solutions[32]. The function of the tightly membrane-bound cyt *c* in normal mitochondria has not been identified. Given that CL-bound cyt *c* cannot act as electron acceptor from respiratory complex III[33], we speculate that catalysis of CL-dependent formation of lipid mediators may represent an unrecognized function of cyt *c*.

For the peroxidase activity of cyt *c*/CL complexes, the presence of sufficient amounts of oxidizing equivalents such as $H_2O_2$ or lipid hydroperoxides ("peroxide tone"[34, 35]) is essential for triggering CL oxidation. Their supply may be driven by disrupted electron transport likely occurring as a consequence of cyt *c* binding with CL[34]. The complex has a redox potential ~400 mV more negative than free cyt *c* – the effect that precludes cyt *c*'s function as an electron acceptor from mitochondrial complex III[33]. As a result accumulating reduced intermediates serve to donate electrons to molecular oxygen yielding superoxide radicals. Spontaneous or catalyzed dismutation of the latter generates $H_2O_2$ that feeds the catalytic peroxidase cycle of cyt *c*/CL complexes. This dependency on $H_2O_2$ as the source of oxidizing equivalents disappears with the accumulation of FA-hydroperoxides or CL-hydroperoxides that can act as more efficient substrates for the peroxidase half-cycle of the process[35].

Cells can express, at different proportions, two isoforms of cyt *c* – s-cyt *c* and t-cyt *c*[21–24]. We found that t-cyt *c* does not significantly contribute to the production of lipid mediators. To investigate if there are potential differences in s-cyt *c* versus t-cyt *c* participation in lipid oxidation, we compared the interaction of two isoforms of cyt *c* with CL using sequence analysis, molecular structural modelling, as well as molecular docking and computational simulations. The sequences of s- and t-cyt *c* and 3D-structures displayed high similarity (Supplementary Fig. S12). Further, ligand docking analysis revealed close similarity between the two isoforms in binding a typical peroxidation substrate, TLCL, as judged by closely matching predicted binding energy values (Supplementary Table S8). Finally, coarse-grained molecular dynamics simulations of cyt *c* interactions with lipid bilayers revealed equally avid binding to TLCL-containing membranes at early stages in the simulation and lack thereof with lipid bilayers devoid of TLCL (Supplementary Fig. S12). This suggests that t-cyt *c*, like s-cyt *c*, should be competent towards peroxidase functions, including CL peroxidation.

The failure of t-cyt *c* to operate as a catalyst of CL oxidation in MECs may mostly due to its presence as apo-protein whereby its biosynthesis into the catalytically active holo-enzyme may be the limiting factor. According to Kim et al., three times more t-cyt *c* was detected by radioimmunoassay, than by spectral assessments of the catalytically competent hemoprotein[36]. Of note, the anti-t-cyt *c* antibody employed in our study does not distinguish between the apo- and holo-proteins. Differences in the localization of these two isoforms of cyt *c* in the intermembrane space and their differential interactions with CLs and other proteins may also be contributory to their dissimilar peroxidase activity towards CLs[37, 38].

The suggested higher pro-apoptotic activity of t-cyt *c* vs s-cyt *c* may be realized through their differential interactions with pro-caspase complexes (Apaf) and the formation of apoptosomes[39].

A notable feature of cyt *c*-catalyzed oxygenation reactions described in this work is accumulation of not only of the expected hydroperoxy-CL and hydroxy-CL[5] but also the presence of epoxy- and oxo-derivatives and truncated products of oxidative cleavage. Whether these derivatives are produced by enzymatic cyt *c*-catalyzed reaction or non-enzymatic process caused by degradation and release of cyt *c*'s heme – is unknown. Similar products require additional enzymatic activities (i.e., epoxidase, epoxide hydrolases) in the traditional pathways triggered by COX and LOX[5]. Our results with pharmacological inhibitors of two different pathways COX/LOX/P450 and (R)-BEL support a role of CL oxidation as a source of the generated lipid mediators. In line with our data, disturbed CL re-acylation in mice with knock-down tafazzin - modeling Barth syndrome - was accompanied by the altered pattern of HETE and oxidized LA and DHA metabolites[40].

The final step in biosynthesis of oxygenated free FAs requires hydrolysis of oxidatively modified CLs by $PLA_2$. Several representatives from different groups of secretory $PLA_2$ ($sPLA_2$) of a large superfamily of $PLA_2$ were shown to display hydrolyzing activity towards peroxidized phospholipids [reviewed in David et al.,[29]]. Among those, the best studied is $LpPLA_2$ – a $Ca^{2+}$-independent $LpPLA_2$ or type VIIA $PLA_2$ - which can be represented by intracellular and secreted forms[30] and is active towards oxygenated long-chain and truncated forms of PC[41]. Oxidized PS has been identified as a representative of anionic peroxidized phospholipids readily hydrolyzable by Lp-$PLA_2$[28].

CLs have been identified as signaling molecules in two major biological functions: mitophagy[42] and apoptosis[11]. In both cases, CL gets externalized to the mitochondrial surface suggesting that any injury to plasma membrane may be associated with the release of these "CL-decorated" mitochondria into extracellular environments. Assuming that apoptosis commonly transitions to necrosis, mitochondria may – with their externalized CL and $CL_{ox}$ – act as damage associated molecular patterns (DAMPs)[26,43]. Our studies reveal that not only CL and $CL_{ox}$ but also $CL_{ox}$ hydrolysis products – mCL and $FFA_{ox}$ – may be released, along with mitochondria, from injured cells. Importantly, sufficient hydrophobicity of mCL retains its association with mitochondria. However, oxygenated mCLs may lose their association with the outer mitochondrial membrane and partition into the aqueous phase of extracellular compartments. Oxygenated FFAs also water-soluble, hence diffuse independently of mitochondrial surfaces. Release of CL[44] and cyt *c*[45] from injured host cells into the extracellular space, have been shown. Thus lipid mediators may also be generated extracellularly from CL with the contribution of cyt *c* and subsequent hydrolysis of $CL_{ox}$ by Lp-$PLA_2$. Overall, CL-dependent lipid mediators may be represented by a diversified variety of membrane-associated and freely diffusible and circulating signaling molecules whose identification and quantitative analysis will represent an intriguing opportunity for the future studies.

Brain has an unprecedented diversification of CLs[13]. By using brain CLs, we showed that a significant variety of lipid mediators could be generated by cyt *c*-catalyzed oxygenation

process. In fact, we found that all eight well known LA-based lipid mediators were generated by cyt *c*/$H_2O_2$ (Supplementary Table S2). In the AA series, we were able to identify nine species of lipid mediators (Supplementary Table S2). A relatively smaller number of oxygenated derivatives of docosapentaenoic acid and DHA were detected in spite of the significant proportion of these FA residues in brain CLs. Also, terminally hydroxylated metabolites of AA, including 17-HETE, 18-HETE, 19-HETE, and 20-HETE were not found, implying that terminal hydroxylation reactions are not catalyzed by cyt *c*/$H_2O_2$ and are likely formed enzymatically after AA liberation.

The ranking order of FA resiues oxidation in the model biochemical system - where all the CL substrates were equally available - was DHA>AA>>LA. The amounts of DHA, AA and LA decreased almost 20-, 5- and 0.3-fold, respectively. The energies for H-abstraction in α-position to bis-allylic double-bonds for different FA with multiple double bonds decrease in the order LA<AA<DHA. Accordingly, the propagation rate constants for FA oxidation determined for LA (one bis-allylic group), AA (3 bis-allylic groups), EPA (4 bis-allylic groups) and DHA (5 bis-allylic groups) increase at ratios of 1, 3.2, 4.0, and 5.4[46]. This is consistent with the assumption that the H-abstraction is essential for oxidation of different polyunsaturated species of CLs by cyt *c*'s protein-immobilized Tyr radical: Tyr-O$^{\bullet}$ +CL-H-> Tyr-OH +CL$^{\bullet}$. Thus, preferential oxidation of LA in brain CL's *in vivo* does not correlate with the chemical reactivity suggesting that CL oxidation in mitochondria is not a simple reaction of CLs with cyt *c*. Availability of CLs for oxidation by cyt *c* in the inter-membrane space likely defines the specificity of the reaction towards different CL species. Our findings with brain CLs may provide a long awaited explanation for a well-known large variety of CL species in the brain and some other tissues (eg, small intestine, lung) – by implying that they are used as precursors for biosynthesis of diversified lipid mediators[47].

In conclusion, we describe a new pathway for generation of lipid mediators. This novel $Ca^{2+}$-independent pathway localizes to mitochondria, involves cyt *c*-catalyzed oxygenation of CL esterified PUFA residues, is followed by hydrolysis of oxygenated CL species by two types of $Ca^{2+}$-independent $PLA_2$ specific towards oxidatively modified phospholipids.

## Methods

This section describes key experiments only; an extended experimental section is provided in the Supplementary Methods.

**Controlled cortical impact** to the left parietal cortex in 17 day old rats was performed as described previously[48]. For all studies, a 6-mm metal pneumatically driven impactor tip was used. The velocity of the impact was 4.0 ± 0.2 m $s^{-1}$, with a penetration depth of 2.5 mm. **Whole body irradiation:** C57BL/6NHsd female mice were irradiated with dose of 10 Gy using a J. L. Shepherd Mark 1 Model 68 cesium irradiator at a dose rate of 80 cGy/min as described previously[49]. 10 Gy of WBI is a LD100/30 for C56Bl6 mice, which means this dose causes death of all animals within 30 days after the exposure. Mice were euthanized 10 or 24 hrs later by $CO_2$ inhalation. All procedures were approved by the IACUC of University of Pittsburgh and performed according to the protocols established.

**Analysis of CL and mCL molecular species** was performed using a Dionex Ultimate™ 3000 HPLC system coupled on-line to a linear ion trap mass spectrometer (LXQ, ThermoFisher Scientific, San Jose, CA) using Luna 3 μm Silica (2) 100 Å column (Phenomenex, Torrance, CA) as described previously[28]. To analyze oxygenated species, CL and mCL were isolated from total lipids by normal phase 2D-HPTLC using mobile phases as described by Rouser et al.,[50]. To prevent lipid oxidation during separation, chromatography was performed under $N_2$ conditions on diethylenetriaminepentaacetic acid (DTPA) treated silica plates (5 × 5 cm, Whatman). CL and mCL were extracted from silica spots[49] and used for reverse phase ESI-LC/MS analysis. LC/MS analysis was performed using a Dionex UltimateTM 3000 RSLCnano system coupled online Q-Exactive hybrid quadrupole-orbitrap mass spectrometer (ThermoFisher Scientific, San Jose, CA) using a $C_8$ column (Luna 3 μm,100 Å, 150 × 2 mm, Phenomenex, Torrance, CA). For $CL_{ox}$ an isocratic solvent system consisting of 2-propanol: water: triethylamine: acetic acid, 45:5:0.25:0.25, v/v was delivered at 150 μl/min for 20 minutes. For $mCL_{ox}$, a gradient of solvent A (acetonitrile: water: triethylamine: acetic acid, 45:5:0.25:0.25 v/v) and B (2-propanol: water: triethylamine: acetic acid, 45:5:0.25:0.25, v/v) was used at the flow rate of 150μl/min as follows: 0–10 min isocratic at 50% solvent B; 10–20 min linear gradient 50–100% solvent B; 20–32 min isocratic at 100% solvent B; 32–35 min linear gradient at 100–50% solvent B; 35–45 min isocratic at 50% solvent B. Spectra were acquired in negative ion mode using a spray voltage of 4.0 kV and a capillary temperature of 320 °C. Scans were acquired in data-dependent mode with an inclusion list for both $CL/CL_{ox}$, $mCL/mCL_{ox}$ species, isolation width of 1.0 Da and a normalized collision energy of 24 in high energy collisional dissociation (HCD) mode. TMCL-$(14:0)_4$ (Avanti Polar Lipids Inc., Alabaster, AL) and mCL-$(14:0)_3$ were used as internal standards. The peaks with signal-to-noise (S/N) ratio of 3 and higher were taken into consideration.

**Detection of oxidized FA.** $LA_{ox}$ was analyzed by LC/MS using a Dionex Ultimate™ 3000 HPLC system coupled on-line to LXQ linear ion trap mass spectrometer (ThermoFisher Scientific, San Jose, CA). A $C_{18}$ column (Luna, 3 μm, 150 × 2 mm, Penomenex, Torrance, CA) and gradient solvents (A: tetrahydrofuran/methanol/water/$CH_3COOH$, 25:30:50:0.1 (v/v/v/v) and B: methanol/water 90:10 (v/v)) containing 5 mM ammonium acetate were used. The column was eluted at a flow rate of 0.2 mL/min during first 3 min isocratically at 50% B, from 3 to 23 min with a linear gradient from 50% solvent B to 98% solvent B, then 23–40 min isocratically using 98% solvent B, 40–42 min with a linear gradient from 98% solvent B to 50% solvent B, 42–28 min isocratically using 50% solvent B for equilibration of the column. Spectra were acquired in negative ion mode using a spray voltage of 5.0 kV and a capillary temperature of 150 °C. Assay method for quantitative assessment of free $AA_{ox}$ and $DHA_{ox}$ was completed as previously described by Miller et al.[51] Briefly, LC was performed using an acuity ultra-performance LC autosampler (Waters, Milford, MA). Separation of analytes was conducted on a UPLC BEH $C_{18}$, 1.7μm (2.1 × 100 mm) column. A gradient mobile phase of 0.005% acetic acid, 5% acetonitrile in deionized water and 0.005% acetic acid in acetonitrile was used with a run time of 6.4 minutes. Analysis was performed using a TSQ Quantum Ultra (ThermoFisher Scientific, San Jose, CA) triple quadrupole mass spectrometer with heated electrospray ionization in negative selective

reaction monitoring mode. Analytical data were acquired and analyzed using Xcalibur software.

## Supplementary Material

Refer to Web version on PubMed Central for supplementary material.

## Acknowledgements

We are thankful to Drs. J.L. Millan and S. Narisawa for providing t-cyt *c*-specific antibody. Supported by NIH: ES020693, ES021068, U19AIO68021, PO1 HL114453, NS076511, NS061817, NS052315; NIOSH OH008282; NCRR S10RR023461, Fulbright U.S/Canada Scholar Program.

## Abbreviations and Textual Footnotes

| | |
|---|---|
| **WBI** | Whole body irradiation |
| **CCI** | controlled cortical impact |
| **COX** | cyclooxygenase |
| **LOX** | lipoxygenase |
| **FA** | fatty acids |
| **$FA_{ox}$** | oxygenated fatty acids |
| **PUFA** | polyunsaturated fatty acids |
| **$PUFA_{ox}$** | oxygenated PUFAs |
| **LA** | linoleic acid |
| **$LA_{ox}$** | oxygenated linoleic acid |
| **AA** | arachidonic acid |
| **$AA_{ox}$** | oxygenated arachidonic acid |
| **EPA** | eicosapentaenoic |
| **DHA** | docosahexaenoic acid |
| **PS** | phosphatidylserine |
| **PE** | phosphatidylethanolamine |
| **PC** | phosphatidylcholine |
| **PI** | phosphatidylinositol |
| **$PIP_2$** | phosphatidylinositol 4,5-bisphosphate |
| **$PLA_2$** | phospholipases $A_2$ |
| **$iPLA_2\gamma$** | $Ca^{2+}$-independent $iPLA_2\gamma$ |
| **$LpPLA_2$** | $Ca^{2+}$-independent lipoprotein-associated $PLA_2$ |
| **PAF-AH** | Platelet activating factor-acetylhydrolase |

| | |
|---|---|
| **CL** | cardiolipin |
| **TMCL** | tetra-linoleoyl-cardiolipin |
| **TLCL** | tetra-mirystoyl-cardiolipin |
| **$TLCL_{ox}$** | oxygenated tetra-linoleoyl-cardiolipin |
| **$CL_{ox}$** | oxygenated cardiolipin species |
| **mCL** | mono-lyso-cardiolipin |
| **$mCL_{ox}$** | oxygenated mono-lyso-cardiolipin |
| **cyt *c*** | cytochrome *c* |
| **s-cyt *c*** | somatic isoform of cytochrome *c* |
| **t-cyt *c*** | testicular isoform of cytochrome *c* |
| **IMM** | inner mitochondrial membrane |
| **OMM** | outer mitochondrial membrane |
| **2D-HPTLC** | two-dimensional high performance thin layer chromatography |
| **MS** | mass spectrometry |
| **LC/MS** | liquid chromatography mass spectrometry |
| **9-KODE** | 9-oxo-octadecadienoic acid |
| **13-KODE** | 13-oxo-octadecadienoic acid |
| **9-HODE** | 9-hydroxy-octadecadienoic acid |
| **13-HODE** | 13-hydroxy-octadecadienoic acid |
| **9,10-EpOME** | 9,10-epoxy-octadecanoic acid |
| **12,13-EpOME** | 12,13-epoxy-octadecanoic acid |
| **9,14-KHODE** | 9-oxo-14-hydroxy-octadecadienoic acid |
| **8,13-HKODE** | 8-hydroxy-13-oxo-octadecadienoic acid |
| **9,12,13-EpKOME** | 9-oxo-12,13-epoxy-octadecanoic acid |
| **8,13-DiHODE** | 8,13-dihydroxy-octadecadienoic acid |
| **8,13-KHpODE** | 8-oxo-13-hydroperoxy-octadecadienoic acid |
| **8,13-HpKODE** | 8-hydroperoxy-13-oxo-9,11-octadecadienoic acid |
| **9,14-KHpODE** | 9-oxo-14-hydroperoxy-octadecadienoic acid |
| **9,14-HpKODE** | 9-hydroperoxy-14-oxo-10,12-octadecadienoic acid |
| **9,12,13-HpEpOME** | 9-hydroperoxy-12,13-epoxy-octadecanoic acid |
| **15-KETE** | 15-oxo-eicosatetraenoic acid |
| **15-HETE** | 15-hydroxy-eicosatetraenoic acid |

| | |
|---|---|
| **12-HETE** | 12-hydroxy- eicosatetraenoic acid |
| **17-HETE** | 17-hydroxy- eicosatetraenoic acid |
| **18-HETE** | 18-hydroxy- eicosatetraenoic acid |
| **19-HETE** | 19-hydroxy- eicosatetraenoic acid |
| **20-HETE)** | 20-hydroxy- eicosatetraenoic acid |

## References


1. Murphy MP. Modulating mitochondrial intracellular location as a redox signal. Science signaling. 2012; 5:pe39. [PubMed: 22990116]
2. Bozza PT, Bakker-Abreu I, Navarro-Xavier RA, Bandeira-Melo C. Lipid body function in eicosanoid synthesis: an update. Prostaglandins Leukot Essent Fatty Acids. 2011; 85:205–213. [PubMed: 21565480]
3. Gutierrez J, Ballinger SW, Darley-Usmar VM, Landar A. Free radicals, mitochondria, and oxidized lipids: the emerging role in signal transduction in vascular cells. Circ Res. 2006; 99:924–932. [PubMed: 17068300]
4. Perez-Chacon G, Astudillo AM, Balgoma D, Balboa MA, Balsinde J. Control of free arachidonic acid levels by phospholipases A2 and lysophospholipid acyltransferases. Biochim Biophys Acta. 2009; 1791:1103–1113. [PubMed: 19715771]
5. Rouzer CA, Marnett LJ. Endocannabinoid oxygenation by cyclooxygenases, lipoxygenases, and cytochromes P450: cross-talk between the eicosanoid and endocannabinoid signaling pathways. Chem Rev. 2011; 111:5899–5921. [PubMed: 21923193]
6. Serhan CN, Chiang N, Van Dyke TE. Resolving inflammation: dual anti-inflammatory and pro-resolution lipid mediators. Nature reviews. Immunology. 2008; 8:349–361.
7. Stables MJ, Gilroy DW. Old and new generation lipid mediators in acute inflammation and resolution. Prog Lipid Res. 2011; 50:35–51. [PubMed: 20655950]
8. Rice GE. Secretory phospholipases and membrane polishing. Placenta. 1998; 19:13–20. [PubMed: 9481780]
9. Vance JE, Tasseva G. Formation and function of phosphatidylserine and phosphatidylethanolamine in mammalian cells. Biochim Biophys Acta. 2013; 1831:543–554. [PubMed: 22960354]
10. Wright MM, Howe AG, Zaremberg V. Cell membranes and apoptosis: role of cardiolipin, phosphatidylcholine, and anticancer lipid analogues. Biochem Cell Biol. 2004; 82:18–26. [PubMed: 15052325]
11. Kagan VE, et al. Cytochrome c acts as a cardiolipin oxygenase required for release of proapoptotic factors. Nat Chem Biol. 2005; 1:223–232. [PubMed: 16408039]
12. Rouzer CA, Marnett LJ. Cyclooxygenases: structural and functional insights. Journal of lipid research. 2009; 50(Suppl):S29–S34. [PubMed: 18952571]
13. Bayir H, et al. Selective early cardiolipin peroxidation after traumatic brain injury: an oxidative lipidomics analysis. Ann Neurol. 2007; 62:154–169. [PubMed: 17685468]
14. Tyurin VA, et al. Mass-spectrometric characterization of phospholipids and their primary peroxidation products in rat cortical neurons during staurosporine-induced apoptosis. Journal of neurochemistry. 2008; 107:1614–1633. [PubMed: 19014376]
15. Yin H, et al. Role of mitochondria in programmed cell death mediated by arachidonic acid-derived eicosanoids. Mitochondrion. 2013; 13:209–224. [PubMed: 23063711]
16. Saab-Aoude S, Bron AM, Creuzot-Garcher CP, Bretillon L, Acar N. A mouse model of in vivo chemical inhibition of retinal calcium-independent phospholipase A2 (iPLA2). Biochimie. 2013; 95:903–911. [PubMed: 23266358]

17. Imig JD, Falck JR, Inscho EW. Contribution of cytochrome P450 epoxygenase and hydroxylase pathways to afferent arteriolar autoregulatory responsiveness. British journal of pharmacology. 1999; 127:1399–1405. [PubMed: 10455289]
18. Liu H, et al. Increased generation of cyclopentenone prostaglandins after brain ischemia and their role in aggregation of ubiquitinated proteins in neurons. Neurotoxicity research. 2013; 24:191–204. [PubMed: 23355003]
19. Rifkind AB, Lee C, Chang TK, Waxman DJ. Arachidonic acid metabolism by human cytochrome P450s 2C8, 2C9, 2E1, and 1A2: regioselective oxygenation and evidence for a role for CYP2C enzymes in arachidonic acid epoxygenation in human liver microsomes. Archives of biochemistry and biophysics. 1995; 320:380–389. [PubMed: 7625847]
20. Laufer SA, Augustin J, Dannhardt G, Kiefer W. (6,7-Diaryldihydropyrrolizin-5-yl)acetic acids, a novel class of potent dual inhibitors of both cyclooxygenase and 5-lipoxygenase. Journal of medicinal chemistry. 1994; 37:1894–1897. [PubMed: 8021931]
21. Narisawa S, et al. Testis-specific cytochrome c-null mice produce functional sperm but undergo early testicular atrophy. Molecular and cellular biology. 2002; 22:5554–5562. [PubMed: 12101247]
22. Vempati UD, et al. Role of cytochrome C in apoptosis: increased sensitivity to tumor necrosis factor alpha is associated with respiratory defects but not with lack of cytochrome C release. Molecular and cellular biology. 2007; 27:1771–1783. [PubMed: 17210651]
23. Vempati UD, Han X, Moraes CT. Lack of cytochrome c in mouse fibroblasts disrupts assembly/stability of respiratory complexes I and IV. The Journal of biological chemistry. 2009; 284:4383–4391. [PubMed: 19075019]
24. Li K, et al. Cytochrome c deficiency causes embryonic lethality and attenuates stress-induced apoptosis. Cell. 2000; 101:389–399. [PubMed: 10830166]
25. Moon SH, et al. Activation of mitochondrial calcium-independent phospholipase A2gamma (iPLA2gamma) by divalent cations mediating arachidonate release and production of downstream eicosanoids. The Journal of biological chemistry. 2012; 287:14880–14895. [PubMed: 22389508]
26. Krysko DV, et al. Emerging role of damage-associated molecular patterns derived from mitochondria in inflammation. Trends in immunology. 2011; 32:157–164. [PubMed: 21334975]
27. Wilensky RL, et al. Inhibition of lipoprotein-associated phospholipase A2 reduces complex coronary atherosclerotic plaque development. Nature medicine. 2008; 14:1059–1066.
28. Tyurin VA, et al. Specificity of lipoprotein-associated phospholipase A(2) toward oxidized phosphatidylserines: liquid chromatography-electrospray ionization mass spectrometry characterization of products and computer modeling of interactions. Biochemistry. 2012; 51:9736–9750. [PubMed: 23148485]
29. David S, Greenhalgh AD, Lopez-Vales R. Role of phospholipase A2s and lipid mediators in secondary damage after spinal cord injury. Cell and tissue research. 2012; 349:249–267. [PubMed: 22581384]
30. Dennis EA, Cao J, Hsu YH, Magrioti V, Kokotos G. Phospholipase A2 enzymes: physical structure, biological function, disease implication, chemical inhibition, and therapeutic intervention. Chem Rev. 2011; 111:6130–6185. [PubMed: 21910409]
31. Daum G, Lees ND, Bard M, Dickson R. Biochemistry, cell biology and molecular biology of lipids of Saccharomyces cerevisiae. Yeast. 1998; 14:1471–1510. [PubMed: 9885152]
32. Kagan VE, et al. Cytochrome c/cardiolipin relations in mitochondria: a kiss of death. Free Radic Biol Med. 2009; 46:1439–1453. [PubMed: 19285551]
33. Basova LV, et al. Cardiolipin switch in mitochondria: shutting off the reduction of cytochrome c and turning on the peroxidase activity. Biochemistry. 2007; 46:3423–3434. [PubMed: 17319652]
34. Belikova NA, et al. Peroxidase activity and structural transitions of cytochrome c bound to cardiolipin-containing membranes. Biochemistry. 2006; 45:4998–5009. [PubMed: 16605268]
35. Belikova NA, et al. Heterolytic reduction of fatty acid hydroperoxides by cytochrome c/cardiolipin complexes: antioxidant function in mitochondria. Journal of the American Chemical Society. 2009; 131:11288–11289. [PubMed: 19627079]

36. Kim IC. Radioimmunoassay for testicular cytochrome c (ct). Evidence for the presence of apocytochrome ct pool in rat testis extract. The Journal of biological chemistry. 1987; 262:11156–11162. [PubMed: 2440885]
37. Schug ZT, Gottlieb E. Cardiolipin acts as a mitochondrial signalling platform to launch apoptosis. Biochim Biophys Acta. 2009; 1788:2022–2031. [PubMed: 19450542]
38. Arnarez C, Marrink SJ, Periole X. Identification of cardiolipin binding sites on cytochrome c oxidase at the entrance of proton channels. Scientific reports. 2013; 3:1263. [PubMed: 23405277]
39. Liu Z, et al. Remarkably high activities of testicular cytochrome c in destroying reactive oxygen species and in triggering apoptosis. Proc Natl Acad Sci U S A. 2006; 103:8965–8970. [PubMed: 16757556]
40. Kiebish MA, et al. Dysfunctional cardiac mitochondrial bioenergetic, lipidomic, and signaling in a murine model of Barth syndrome. Journal of lipid research. 2013; 54:1312–1325. [PubMed: 23410936]
41. Davis B, et al. Electrospray ionization mass spectrometry identifies substrates and products of lipoprotein-associated phospholipase A2 in oxidized human low density lipoprotein. The Journal of biological chemistry. 2008; 283:6428–6437. [PubMed: 18165686]
42. Chu CT, et al. Cardiolipin externalization to the outer mitochondrial membrane acts as an elimination signal for mitophagy in neuronal cells. Nature cell biology. 2013; 15:1197–1205. [PubMed: 24036476]
43. Garg AD, et al. Immunogenic cell death, DAMPs and anticancer therapeutics: an emerging amalgamation. Biochim Biophys Acta. 2010; 1805:53–71. [PubMed: 19720113]
44. Ray NB, et al. Dynamic regulation of cardiolipin by the lipid pump Atp8b1 determines the severity of lung injury in experimental pneumonia. Nature medicine. 2010; 16:1120–1127.
45. Codina R, Vanasse A, Kelekar A, Vezys V, Jemmerson R. Cytochrome c-induced lymphocyte death from the outside in: inhibition by serum leucine-rich alpha-2-glycoprotein-1. Apoptosis : an international journal on programmed cell death. 2010; 15:139–152. [PubMed: 19851871]
46. Xu L, Davis TA, Porter NA. Rate constants for peroxidation of polyunsaturated fatty acids and sterols in solution and in liposomes. Journal of the American Chemical Society. 2009; 131:13037–13044. [PubMed: 19705847]
47. Cheng H, et al. Shotgun lipidomics reveals the temporally dependent, highly diversified cardiolipin profile in the mammalian brain: temporally coordinated postnatal diversification of cardiolipin molecular species with neuronal remodeling. Biochemistry. 2008; 47:5869–5880. [PubMed: 18454555]
48. Ji J, et al. Lipidomics identifies cardiolipin oxidation as a mitochondrial target for redox therapy of brain injury. Nature neuroscience. 2012; 15:1407–1413. [PubMed: 22922784]
49. Tyurina YY, et al. Oxidative lipidomics of gamma-radiation-induced lung injury: mass spectrometric characterization of cardiolipin and phosphatidylserine peroxidation. Radiation research. 2011; 175:610–621. [PubMed: 21338246]
50. Rouser G, Fkeischer S, Yamamoto A. Two dimensional then layer chromatographic separation of polar lipids and determination of phospholipids by phosphorus analysis of spots. Lipids. 1970; 5:494–496. [PubMed: 5483450]
51. Miller TM, et al. Rapid, simultaneous quantitation of mono and dioxygenated metabolites of arachidonic acid in human CSF and rat brain. J Chromatogr B Analyt Technol Biomed Life Sci. 2009; 877:3991–4000.

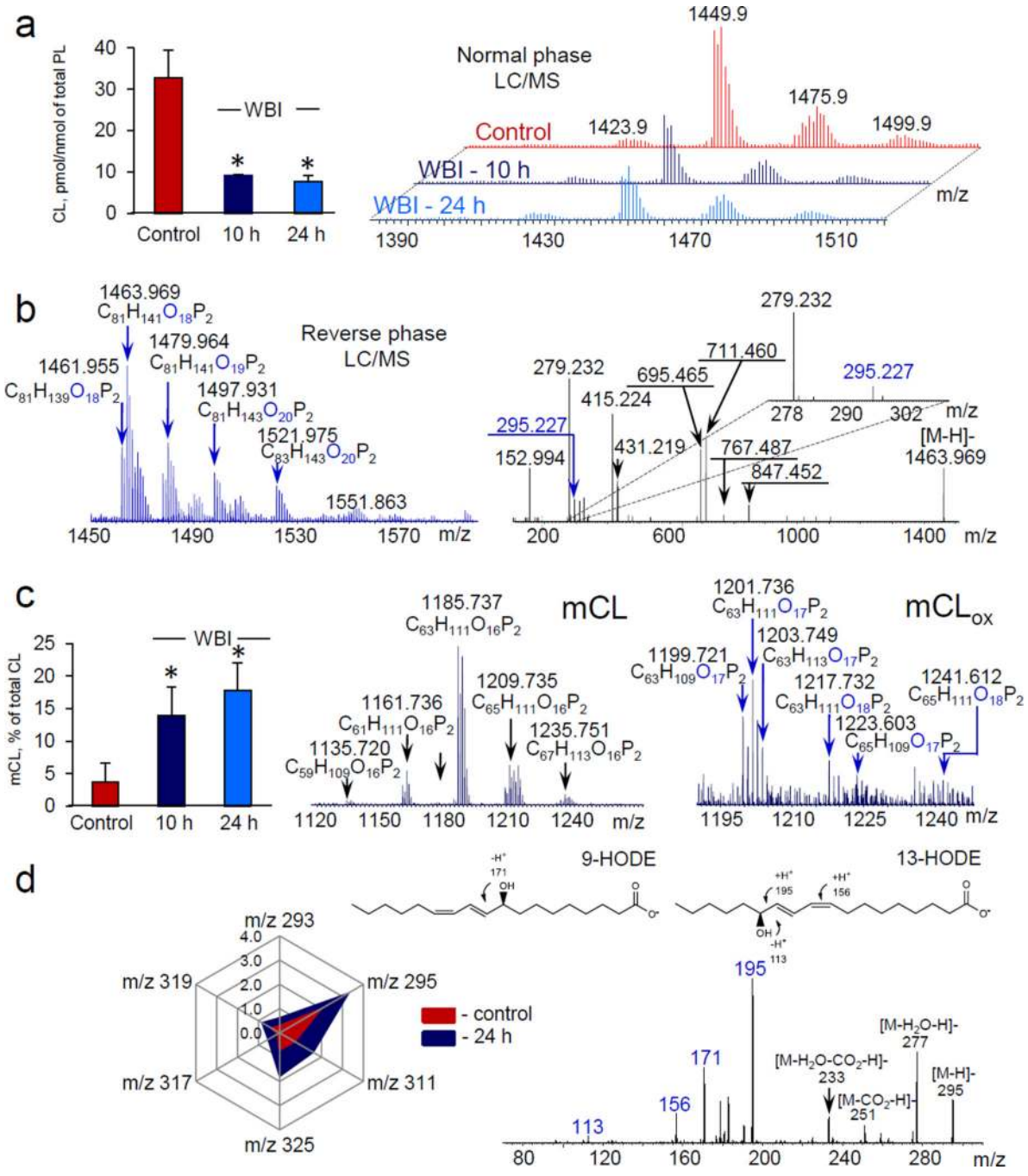


**Figure 1. Exposure of mice to whole body irradiation (WBI) causes cardiolipin (CL) oxidation and accumulation of its hydrolysis products in small intestine**

**a,** Quantitation of polyunsaturated CL (left) and MS spectra of CL before and after WBI (10 Gy) (right). Each cluster included 4–5 signals with differing m/z. **b,** Typical MS spectrum of oxidized CL ($CL_{ox}$) obtained 10 hrs after WBI (left) and fragmentation pattern of molecular ion with m/z 1463.969 containing oxygenated linoleic acid ($LA_{ox}$) (m/z 295.227). **c,** Quantitation of total monolyso-CL (mCL) (left), MS spectra of mCL (middle) and oxygenated mCL ($mCL_{ox}$) (right). Both mono- and di-oxygenated molecular species of

$mCL_{ox}$ were detected 10 hrs after WBI, whereby the mono-oxygenated mCL species were predominant. **d,** Quantitation of oxygenated polyunsaturated fatty acids ($PUFA_{ox}$) (left) accumulated after WBI and MS/MS spectrum of molecular ion with m/z 295 (right). Data are presented as pmol/nmol of total phospholipids. Molecular species of $PUFA_{ox}$ were represented by $LA_{ox}$ with m/z 293 (13-KODE, 9-KODE); m/z 295 (13-HODE, 9-HODE, 9,10-EpOME, 12,13-EpOME); m/z 311 (9-HpODE, 8,13-DiHODE); m/z 325 (9,14-KHpODE, 9,14-HpKODE, 8,13-KHpODE, 8,13-HpKODE) and oxygenated arachidonic acid with m/z 319 (12-HETE) and m/z 317 (15-KETE). Data are means ± S.D., $*p < 0.05$ *vs* control, n=5.

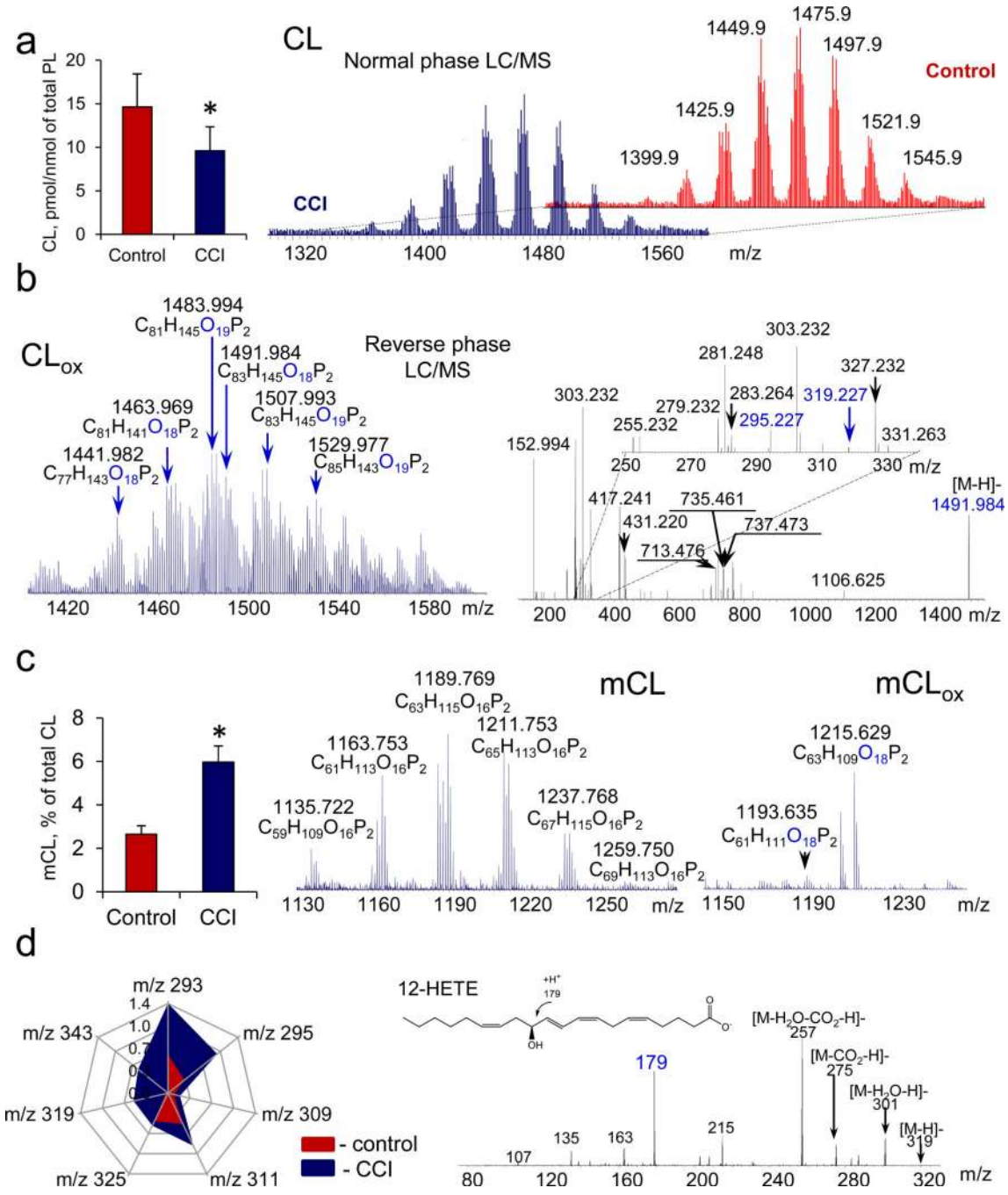


**Figure 2. Exposure of rats to controlled cortical impact (CCI) causes cardiolipin (CL) oxidation and accumulation of its hydrolysis products in brain**

**a,** Quantitation of polyunsaturated CL (left) and MS spectra of CL in control and 3 hrs after CCI (right). The spectrum of brain CLs includes nine major clusters of signals with 8–9 components with differing m/z in each. **b,** Typical MS spectrum of oxidized CL ($CL_{ox}$) (left) and fragmentation pattern of $CL_{ox}$ molecular ion with m/z 1491.984 (right) represented by two species containing either oxygenated linoleic acid ($LA_{ox}$) (m/z 295.227) or arachidonic acid ($AA_{ox}$) (m/z 319.227) and originated from m/z 1475.980. **c,** Quantitation

of total monolyso-CL (mCL) (left) and MS spectra of mCL (middle) and oxygenated mCL ($mCL_{ox}$) (right) formed after CCI. Di-oxygenated species of $mCL_{ox}$ were detected in injured brain. **d,** Quantitation of major polyunsaturated fatty acids (left) and MS/MS spectrum of molecular ion with m/z 319 (right). Data are presented as pmol/nmol of total phospholipids. Species of $LA_{ox}$ with m/z 293 (13-KODE, 9-KODE); m/z 295 (13-HODE, 9-HODE, 9,10-EpOME, 12,13-EpOME); m/z 311 (9-HpODE, 8,13-diHODE), m/z 309 (8,13-HKODE, 9,14-KHODE); m/z 325 (9,14-KHpODE, 9,14-HpKODE, 8,13-KHpODE, 8,13-HpKODE) and $AA_{ox}$ with m/z 319 (12-HETE,15-HETE) were identified. Small amounts of $DHA_{ox}$ (m/z 343) were also detected. Data are means ± S.D., $*p < 0.05$ *vs* control, n=4.

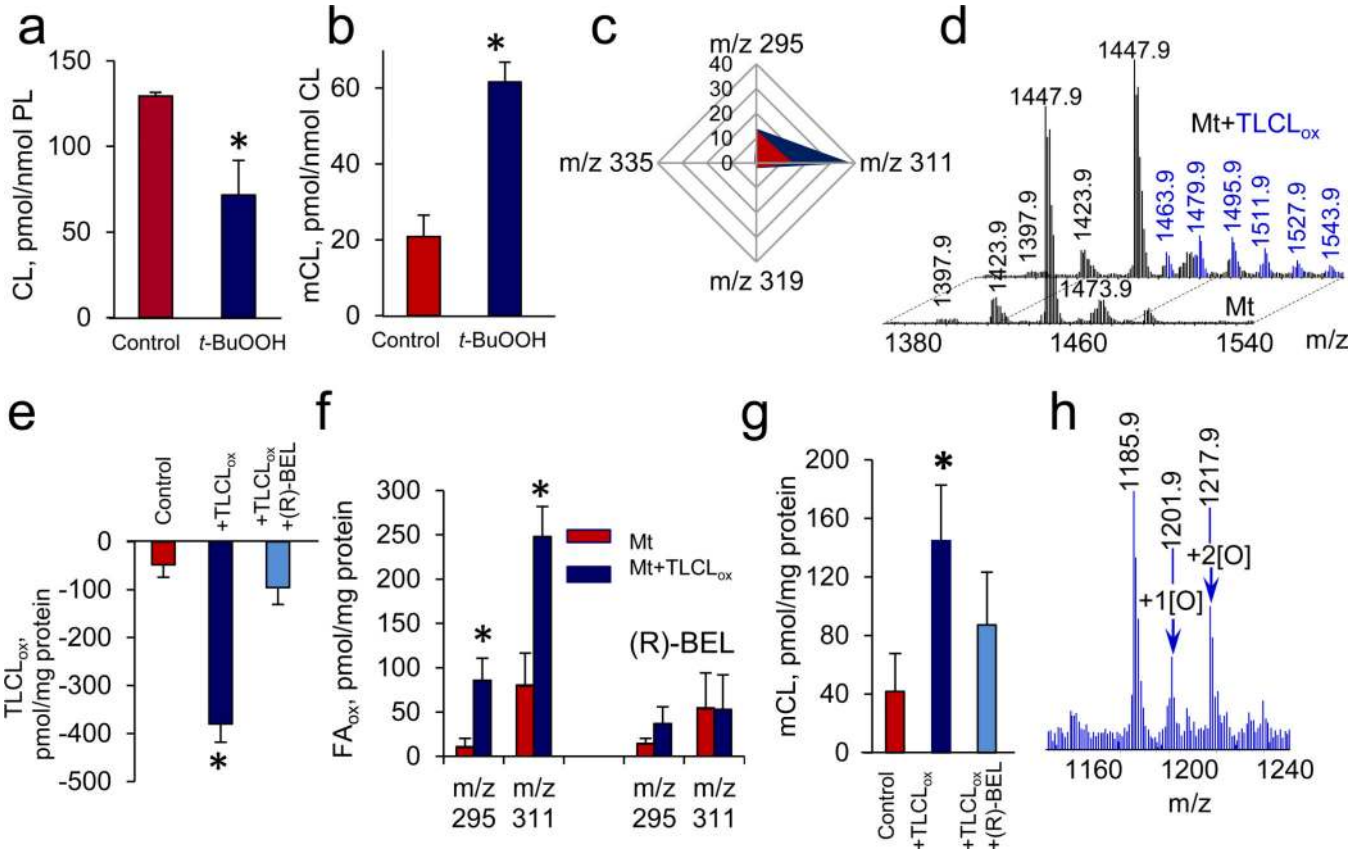


**Figure 3. Peroxidized cardiolipins (CL) undergo phospholipase $A_2$-catalyzed hydrolysis in mitochondria**

**a, b, c,** Oxidation of CL (a) and accumulation of monolyso-CL (mCL) (b) and oxygenated fatty acids ($FA_{ox}$) (c) in mouse heart mitochondria treated with *t*-BuOOH (150 μM). Oxygenated linoleic acid (m/z 295 and m/z 311) and oxygenated arachidonic acid (m/z 319 and 335) containing one and two oxygens were detected. Data are presented as pmols $FA_{ox}$ per nmol of phospholipids. Data are means ± S.D., *$p < 0.05$ vs. control, n = 3. **d,e,f,g,h,** Effect of 6E-(bromoethylene)tetrahydro-3R-(1-naphthalenyl)-2H-pyran-2-one, (R)-bromoenol lactone) (R)-BEL, $Ca^{2+}$-independent $iPLA_2\gamma$ inhibitor, on hydrolysis of exogenous oxidized tetra-linoleyl CL ($TLCL_{ox}$) by mouse liver mitochondria. MS spectra of CL obtained from mouse liver mitochondria before and after addition of $TLCL_{ox}$ (d). TLCL was oxidized by cyt c/$H_2O_2$ (see Supplementary Fig.S10). Content of $TLCL_{ox}$ (e), $FA_{ox}$ (f) and mCL (g) in mitochondria incubated with exogenous $TLCL_{ox}$ in the presence and in the absence of (R)-BEL. MS spectrum of mCL from mitochondria incubated in the presence of $TLCL_{ox}$ (h). Data are mean ± S.D., *$p < 0.05$ vs. non-treated mitochondria, n=3.

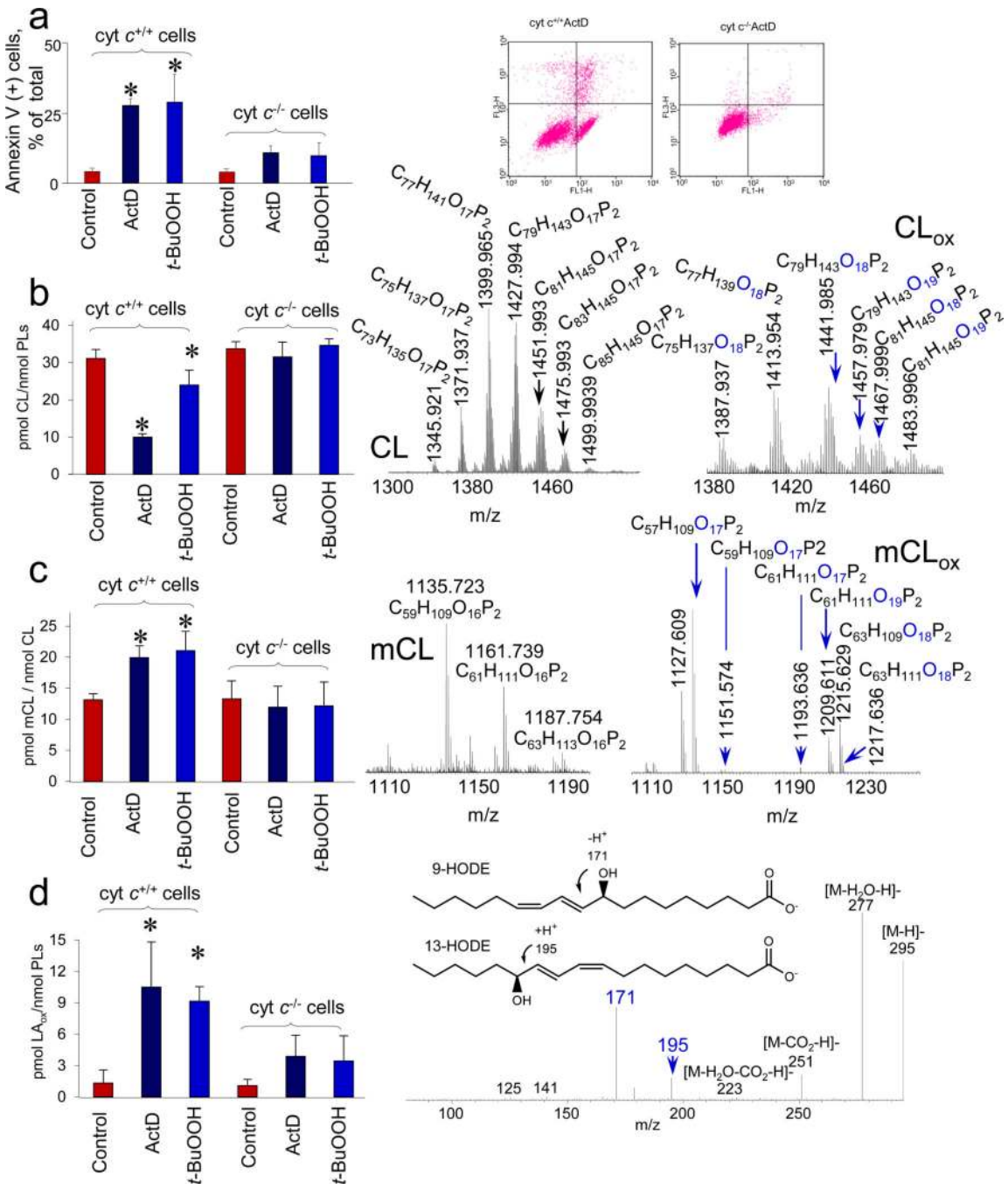


**Figure 4. Execution of apoptosis is accompanied by cardiolipin (CL) oxidation and accumulation of its hydrolysis products in mouse embryonic cyt $c^{+/+}$ (but not cyt $c^{-/-}$) cells**

**a,** Assessments of a biomarker of apoptosis, externalized phosphatidylserine, in cyt $c^{+/+}$ and cyt $c^{-/-}$ cells by annexin V binding (left). Flow cytometry data from a representative experiment after treatment of cells with ActD (100 ng/mL, 16 hrs): the number of annexin V/FITC-positive cells is shown in log scale (right). **b)** Consumption of CL in either ActD or *t*-BuOOH (200 μM, 16 hrs) treated cyt $c^{+/+}$ and cyt $c^{-/-}$ cells (left) and MS spectra of CL (middle), oxygenated CL ($CL_{ox}$) (right) from cyt $c^{+/+}$ cells exposed to ActD. **c,**

Accumulation of monolyso-CL (mCL) in either ActD or *t*-BuOOH treated cyt $c^{+/+}$ and cyt $c^{-/-}$ cells (left) and MS spectra of mCL (middle), oxygenated mCL ($mCL_{ox}$) (right) from cyt $c^{+/+}$ ActD treated cells. **d,** Accumulation of oxygenated linoleic acid ($LA_{ox}$) in ActD and *t*-BuOOH treated cyt $c^{+/+}$ and cyt $c^{-/-}$ cells (left) and MS/MS fragmentation pattern of $LA_{ox}$ (m/z 295) (right) formed in ActD treated cyt $c^{+/+}$ cells. Mono-oxygenated $LA_{ox}$ was predominantly accumulated and represented by both 9-HODE and 13-HODE. Data are mean ± S.D., $^{*}p < 0.01$ vs control, n=3–4.

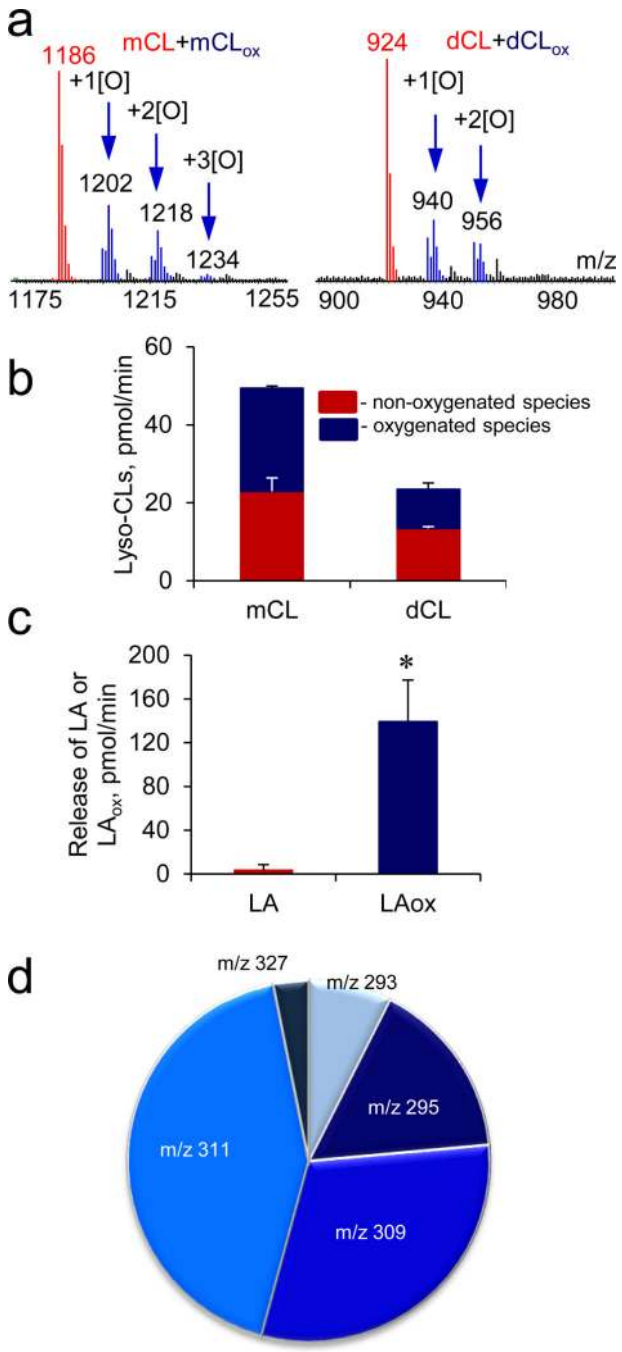


**Figure 5. Platelet activating factor-acetylhydrolase (PAF-AH) catalyzes hydrolysis of oxygenated tetra-linoleyl-CL (TLCL)**

**a,** MS spectra of monolyso-CLs (mCLs) (left) and dilyso-CLs (dCLs) (right) formed during PAF-AH-driven hydrolysis of oxygenated TLCL ($TLCL_{ox}$). Arrows show oxygenated mCL ($mCL_{ox}$) and dCL ($dCL_{ox}$) species (and their m/z values) with indicated oxygen atoms added. **b, c,** Quantitative assessment of lyso-CLs (b), non-oxygenated and oxygenated linoleic acid ($LA_{ox}$) (c) formed during PAF-AH-driven hydrolysis of $TLCL_{ox}$. **d,** Identification and quantification of $LA_{ox}$ liberated after hydrolysis of $TLCL_{ox}$ by PAF-AH.

Molecular ions of $LA_{ox}$ with m/z 293 (13-KODE, 9-KODE), m/z 295 (13-HODE, 9-HODE, 9,10-EpOME, 12,13-EpOME), m/z 309 (8,13-HKODE, 9,14-KHODE), m/z 311 (9-HpODE, 13-HpODE and 8,13-DiHODE) and m/z 327 (9,12,13-HpEpOME) were detected. Data are means ± S.D., $*p < 0.05$ vs. LA, n=4.

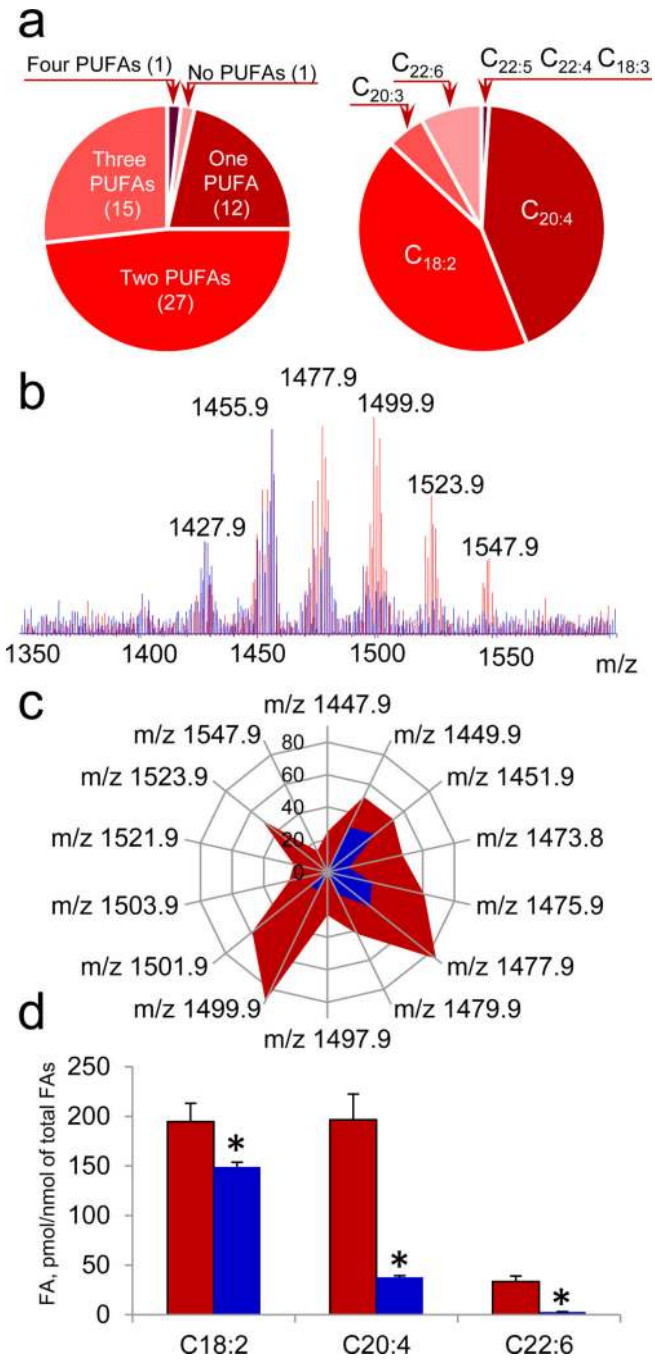


**Figure 6. Cytochrome *c* (cyt *c*)/$H_2O_2$ induces oxidation of polyunsaturated fatty acid (PUFA) residues of cardiolipin (CL) isolated from mouse brain**

**a,** Characterization of polyunsaturated fatty acids (PUFA) esterified to brain CL. Number of CL molecular species containing PUFA (left). PUFA distribution in brain CL species (right). **b, c,** MS spectra (b) and quantitative assessment of brain CL molecular species (c) obtained before (red) and after (blue) treatment with cyt *c* in the presence of $H_2O_2$. **d,** Quantitative assessment of PUFA of non-oxidized CL (red) and CL exposed to cyt *c*/$H_2O_2$ (blue). *$p$ < 0.05 *vs* control (CL not treated with cyt *c*). Data are means ± S.D., n=3.